Zoosyst. Evol. 102 (2) 2026, 659–670 | DOI 10.3897/zse.102.181212

PENSOFT

für Natur MUSEUM FÜR NATURKUNDE BERLIN

# A new species of the genus *Typhlomys* Milne-Edwards, 1877 (Rodentia, Platacanthomyidae) from Fanjing Mountain, Guizhou, China

Tao Zhang[1], Zhengkun Hu[2], Qingfang Zou[1], Lin Gu[1], Wei Zhuang[1], Pengxi Gu[1], Jiali Zhan[1], Xiaoqi Mi[3], Shaoying Liu[4], Shunde Chen[1]

1 *College of Life Sciences, Sichuan Normal University, Chengdu 610066, China*

2 *Administrative Bureau of Fanjingshan National Nature Reserve, Jiangkou 554400, Guizhou, China*

3 *College of Agriculture and Forestry Engineering and Planning, Guizhou Provincial Key Laboratory of Biodiversity Conservation and Utilization in the Fanjing Mountain Region, Tongren University, Tongren, Guizhou, 554300, China*

4 *Sichuan Academy of Forestry, Chengdu 610081, China*

*https://zoobank.org/4D2B299F-3746-4E52-AFBE-35FD28624A0E*

Corresponding authors: Shaoying Liu (Shaoyliu@163.com); Shunde Chen (csd111@126.com)

Academic editor: Melissa T. R. Hawkins ♦ **Received** 4 December 2025 ♦ **Accepted** 19 March 2026 ♦ **Published** 8 April 2026

## Abstract

During a field survey of small mammals on Fanjing Mountain in Guizhou Province, China, we collected five specimens of *Typhlomys*. To assess their taxonomic status, we performed phylogenetic analyses using three mitochondrial genes (*Cytb*, *COI*, and *ND2*) and two nuclear genes (*GHR* and *IRBP*). We also compared the cranial and dental morphology of these specimens with those of other known *Typhlomys* species. Our results indicate that the specimens represent a new species, described herein as *Typhlomys zhengkuni* **sp. nov.** Phylogenetic analyses suggest that the new species forms a distinct clade sister to *T. taxuansis*. The Kimura 2-parameter (K2P) genetic distances based on *Cytb* between the new taxon and other species of *Typhlomys* ranged from 8.2% to 17.9%, supporting its status as a distinct lineage. Morphologically, *Typhlomys zhengkuni* **sp. nov.** is most similar to *T. daloushanensis* but can be distinguished by its lower molars. However, given the low nodal support for its sister relationship with *T. taxuansis*, the precise phylogenetic position of this new species requires further investigation using additional molecular markers and specimens.

## Key Words

Genus *Typhlomys*, morphology, new species, phylogenetics

## Introduction

The genus *Typhlomys* Milne-Edwards, 1877 (Rodentia, Platacanthomyidae) comprises rodents predominantly distributed in southern China and northern Vietnam (Musser and Carleton 2005; Abramov et al. 2012). Commonly known as "blind mice" due to their notably small eyes, these animals also possess morphological traits such as large ears, long tails, and elongated hind feet, which are adaptations that likely facilitate their nocturnal and arboreal lifestyle (Smith 2008). Recently, they have been identified as a newly discovered echolocating lineage within mammals (He et al. 2021).

For years, the taxonomy of the genus *Typhlomys* was considered monotypic, comprising only *Typhlomys cinereus* (first described by Milne-Edwards in 1877) with several subspecies (Wang 1996). However, Chen et al. (2017) revealed substantial divergence within the genus based on molecular and morphological analyses, which is further corroborated by subsequent studies (Su et al. 2020). In recent years, multiple new species of *Typhlomys* have been described (Hu et al. 2021; Pu et al. 2022; Balakirev et al. 2024). Currently, seven species of *Typhlomys* are recognized: *T. cinereus*, *Typhlomys chapensis* (Abramov et al. 2014), *Typhlomys daloushanensis* (Wang and Li 1996), *Typhlomys nanus* (Chen et al. 2017), *Typhlomys huangshanensis* (Hu and Zhang

Copyright *Zhang, T. et al.* This is an open access article distributed under the terms of the Creative Commons Attribution License (CC BY 4.0), which permits unrestricted use, distribution, and reproduction in any medium, provided the original author and source are credited.

2021), *Typhlomys fengjiensis* (Pu et al. 2022), and *Typhlomys taxuansis* (Balakirev et al. 2024). In addition, one candidate species (*Typhlomys* sp. 2 from earlier studies) and one putative species (samples from Libo, Guizhou, described in Su et al. 2020; Pu et al. 2022) await further confirmation.

During recent fieldwork (2024–2025), we collected five *Typhlomys* specimens from Fanjing Mountain in Guizhou Province, China. Preliminary molecular analyses indicate that these individuals are genetically distinct from all recognized species in the genus; we therefore provisionally refer to this lineage as *Typhlomys* sp. 1. In this study, we integrated molecular and morphometric approaches to evaluate the taxonomic status of these specimens.

## Materials and methods

A total of five individuals (*Typhlomys* sp. 1) were collected using snap traps placed in forests and near stone piles on Fanjing Mountain, Guizhou, China (Fig. 1, Suppl. material 5: fig. S1D). Fresh muscle and liver tissues were taken from each specimen, preserved in 95% ethanol, and stored at −80 °C for subsequent molecular analyses. All voucher specimens and associated tissue samples have been deposited in the Zoological Collection of the College of Life Sciences, Sichuan Normal University (SCNU).

A total of 76 specimens of *Typhlomys* were used for morphological analysis, including *T. cinereus* ($N = 2$), *T. daloushanensis* ($N = 29$), *T. chapensis* ($N = 21$), *T.* nanus ($N = 3$), *T. fengjiensis* ($N = 7$), *T. huangshanensis* ($N = 9$), and five specimens of *Typhlomys* sp. 1. External measurements (including body mass (BM), head-body length (HBL), tail length (TL), hind foot length (HL), and ear length (EL)) were excluded from the analysis because BM may be influenced by nutritional status and reproductive status and is less stable for taxonomic comparison in this study, while measurements (HBL, TL, HL, and EL) are likely to show considerable inter-observer variability (Jiang and Hoffmann 2001). Eleven craniodental metrics were measured using a digital caliper graduated to 0.01 mm, following Yang et al. (2005), Xia et al. (2006), and Cheng et al. (2017). The morphological characters of the skull and their abbreviations are the greatest length of skull (GLS), condylobasal length (CBL), basal length (BL), braincase height (BCH), zygomatic width (ZMW), interorbital breadth (IOB), length between the upper incisors and molars (LUIM), crown breadth of the first upper molars (M1–M1), length of the upper molar row (UML), length between the backmost notch point of the mandible and front of lower molars (LNM–FLM), and height of the coronoid valley (HCV). Cranial measurements of 71 recognized *Typhlomys* individuals were obtained from previous studies (Cheng et al. 2017; Hu et al. 2021; Pu et al. 2022). *Typhlomys* sp. 2 and *T. taxuansis* were not included in the morphological analysis. The measurements of the skull were analyzed using SPSS v. 26.0 (SPSS, Chicago, IL, USA) for principal component analysis (PCA) and canonical discriminant function analysis (DFA). The terminology for morphological descriptions followed Cheng et al. (2017), Hu et al. (2021), and Pu et al. (2022).

Total genomic DNA was extracted from muscle or liver tissues using an animal tissue DNA extraction kit (Chengdu Fuji Biotechnology Co., Ltd., Sichuan, China). We amplified three mitochondrial genes (i.e., cytochrome b gene (*Cytb*, 1000 bp), cytochrome c oxidase subunit I (*COI*, 1400 bp), and NADH dehydrogenase subunit 2 (*ND2*, 1045 bp)) and two nuclear genes (i.e., growth hormone receptor (*GHR*, 919 bp) and interphotoreceptor retinoid-binding protein (*IRBP*, 1202 bp)). Polymerase chain reaction (PCR) was performed using the primers and cycling conditions as described in Cheng et al. (2017) and Pu et al. (2022) (detailed in Suppl. material 4). All DNA sequences were edited with EditSeq (DNASTAR, Lasergene v. 7.1) and further aligned in MEGA 11 (Tamura et al. 2021). Corresponding sequences of published *Typhlomys* individuals and sequences of outgroups were obtained from GenBank (Suppl. material 1).

We performed Bayesian inference (BI) analysis to reconstruct the phylogenetic relationships using MrBayes 3.2.7 (Ronquist 2012) in PhyloSuite v. 1.2.3 (Zhang et al. 2020). Three datasets were constructed for phylogenetic analysis: (1) concatenated mitochondrial genes (*Cytb* + *COI* + *ND2*), (2) concatenated nuclear genes (*GHR* + *IRBP*), and (3) concatenated mitochondrial and nuclear genes (mtDNA + nuDNA). ModelFinder v. 2.20 was used to determine the optimal model for each gene, and the fitness of the model was estimated using the Bayesian Information Criterion (BIC). Each run was performed using four Markov chain Monte Carlo (MCMC) algorithms, with 10,000,000 generations for all datasets. IQ-TREE (Nguyen et al. 2015) was used for maximum likelihood (ML) analyses based on three datasets, with 10,000 ultrafast bootstraps to estimate branch support. Posterior probabilities (PP) > 95% and ultrafast bootstrap values (UFBoot) ≥ 95 were considered to be strongly supported (Huelsenbeck and Rannala 2004; Minh et al. 2018).

The Poisson tree processes (PTP) model was used to infer putative species boundaries on the concatenated gene (*Cytb* + *GHR*) ML phylogenetic input tree, which was conducted in the online bPTP server available at http://species.h-its.org/ptp (Zhang et al. 2013). Bayesian Phylogenetics and Phylogeography (BPP) analyses were performed using two datasets (*IRBP* + *GHR*) and concatenated mitochondrial and nuclear genes (mtDNA + nuDNA) in BPP v3.1 (Yang and Rannala 2010). Following Chen et al. (2022), we used two alternative rjMCMC algorithms (algorithms 0 and 1). The ancestral population size and root age were represented by $\theta$ and $\tau$, respectively. Three combination priors on $\theta$ and $\tau$ were adopted: (1) G (1, 10) for $\theta$ and G (1, 10) for $\tau$, (2) G (1, 10) for $\theta$ and G (2, 2000) for $\tau$, (3) G (2, 2000) for $\theta$ and G (2, 2000) for $\tau$. Each rjMCMC was run for 100,000 generations and sampled every 100 generations after discarding 10,000 generations as pre-burn-in. Each clade was supported as an independent species if the posterior probability was greater than 0.95.

The Kimura-2-parameter (K2P) distances for species and putative species based on the *Cytb* gene were calculated in MEGA 11 (Kimura 1980; Tamura et al. 2021).

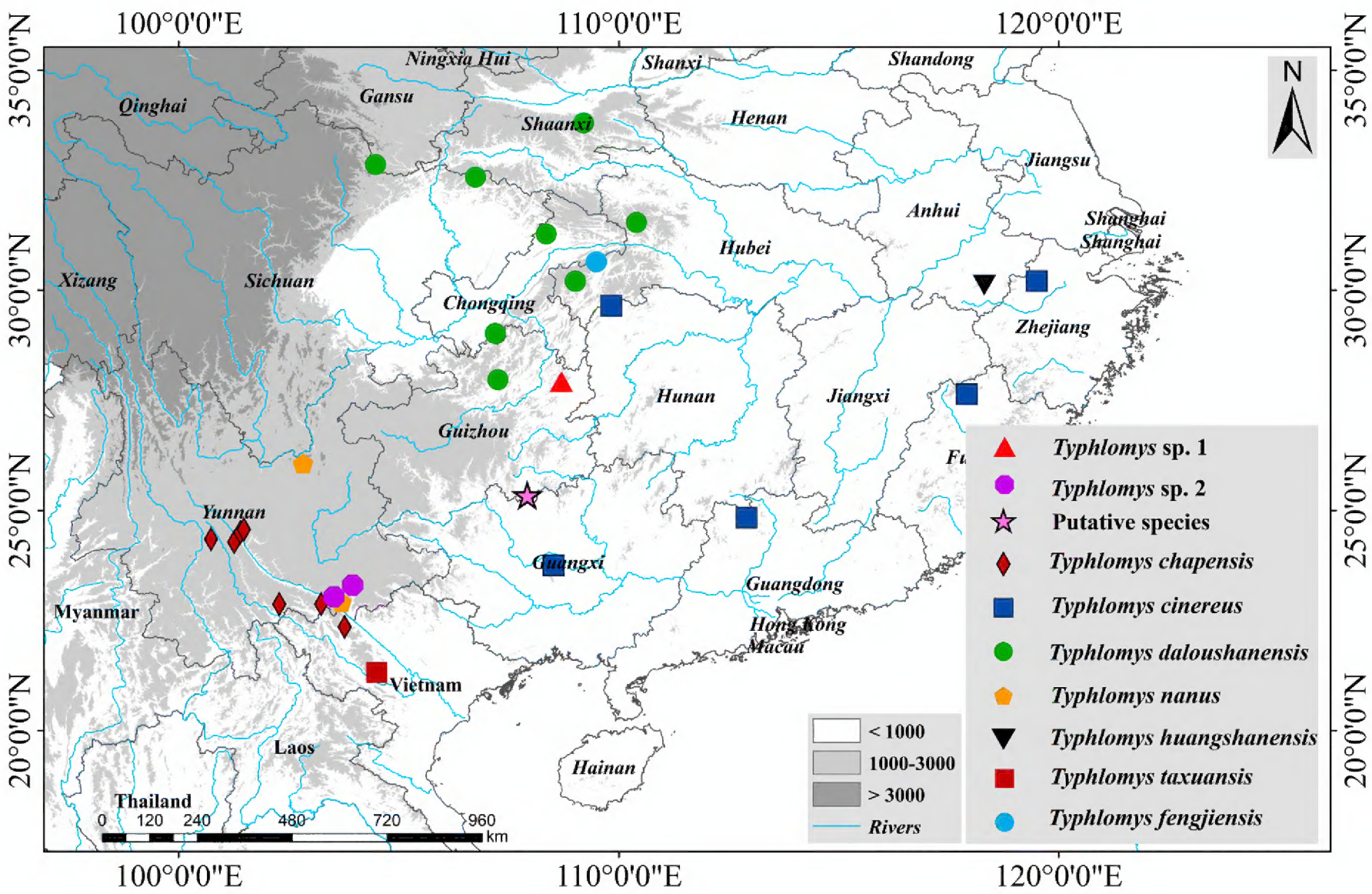


**Figure 1.** Sample localities of the genus *Typhlomys*. Distribution ranges are shown as colored polygons for each species (see legend); data for all except *Typhlomys* sp. 1 are from Chen et al. (2017), Pu et al. (2022), and Balakirev et al. (2024), with detailed coordinates provided in Suppl. material 1. Elevation is shown with a grayscale: white (<1,000 m), light gray (1,000–3,000 m), and dark gray (>3,000 m). Regional names are placed near their geographic centers. The red triangle marks the collection site of the new species (*Typhlomys* sp. 1) on Fanjing Mountain, Guizhou, China. Two candidate species, *Typhlomys* sp. 2, and a putative species from Libo were described in earlier studies (Su et al. 2020; Pu et al. 2022).

We used the concatenated mtDNA and nuDNA genes dataset to estimate divergence times in BEAST 2.6 (Bouckaert et al. 2014). Two fossil calibration points were used following Pu et al. (2022): (1) the earliest known member of the crown clade of Muroidea and Dipodidae (Rodrigues et al. 2010) at approximately 54 Ma was used as the split of the most recent common ancestor of all taxa, and we set up the prior using an exponential distribution; the mean age was set at 54 Ma and 17.82 for the offset (offset = 17.82, mean = 54). (2) The minimum age and the mean value of the exponential distribution probability were set at 45 Ma and 4.64, respectively (offset = 45, mean = 4.64). The BEAST analysis used a Birth-Death tree prior and a relaxed lognormal clock model. Each analysis ran for 100 million generations and was sampled every 5,000 generations. The posterior distribution and ESS of each parameter higher than 200 were calculated in Tracer v. 1.7 (Rambaut et al. 2018). TreeAnnotator v. 1.6.1 was used to determine the necessary burn-in fraction, which was set to the first 25% of the generations.

## Results

The external and cranial measurements of *Typhlomys* are shown in Table 1. Results of the Kaiser–Meyer–Olkin measure of sampling adequacy indicated that the data were suitable for PCA (KMO = 0.877, Bartlett's test <0.001). The PCA based on 11 craniodental measurements of 76 individuals extracted two principal components (PC1 and PC2; Table 2), with eigenvalues > 1.0. PC1 explained 65.448% of the total variation (eigenvalues = 7.199), which was primarily loaded by GLS, LUIM, BL, M1–M1, CBL, ZMW, LNM–FLM, HCV, and UML. PC2 explained 12.906% of the total variation (eigenvalues = 1.420), dominated by IOB and BCH. The scatterplots of PCA (Fig. 2A) showed that *T. daloushanensis*, *Typhlomys* sp. 1, and *T. fengjiensis* specimens occupied the positive region of PC1. *Typhlomys* sp. 1 and *T. fengjiensis* also occupied the positive region on PC2, with the majority of *T. chapensis* and part of *T. daloushanensis*. *T. nanus*, *T. huangshanensis*, and one *T. cinereus* sample were in the negative fields of PC1 and PC2. Moreover, all species exhibited good separation, except for *Typhlomys* sp. 1, *T. fengjiensis*, and *T. daloushanensis*, which showed partial overlap. Discriminant function analysis of the same variables correctly classified 98.7% of morphometric distinctions. One *Typhlomys* sp. 1 sample was assigned to *T. fengjiensis*. Plots of CAN1 and CAN2 (Fig. 2B) showed that most species separated well, and the three groups (*Typhlomys* sp. 1, *T. fengjiensis*, and *T. daloushanensis*) separated from each other, while *Typhlomys* sp. 1 and *T.* fengjiensis exhibited partial overlap. Canonical axes (CAN) 1–6 explained 51.5%, 27.50%, 16.6%, 2.90%, 1%, and 0.5% of the total variation, respectively (Table 2).

**Table 1.** External and cranial morphological measurements (mm) of *Typhlomys*.

| Variable | *T. cinereus* (n = 2) | *T. daloushanensis* (n = 29) | *T. chapensis* (n = 21) | *T. nanus* (n = 3) | *T. huangshanensis* (n = 9) | *T. fengjiensis* (n = 7) | *Typhlomys* sp.1 (n = 5) |
|---|---|---|---|---|---|---|---|
| BM | / | 22.98 ± 3.68 | 16.93 ± 3.58 | 10.47 ± 2.39 | 15.33 ± 2.50 | 25.54 ± 5.99 | 26.48 ± 3.33 |
| | / | 15.40–31.00 | 7.70–22.60 | 8.80–13.20 | 12.03–20.40 | 19.35–34.60 | 21.70–31.20;5 |
| TL | 99.00 ± 4.24 | 116.80 ± 5.35 | 106.00 ± 1.45 | 102.00 ± 4.58 | 98.87 ± 5.11 | 123.00 ± 4.40 | 120.40 ± 5.78 |
| | 96.00–102.00 | 105.00–129.00 | 80.00–126.00 | 97.00–106.00 | 91.00–107.00 | 114–127 | 113–129;5 |
| HB | 73.50 ± 3.54 | 86.05 ± 6.55 | 77.59 ± 10.87 | 70.00 ± 4.58 | 77.49 ± 4.69 | 89.86 ± 8.76 | 84.2 ± 8.52 |
| | 71.00–76.00 | 72.00–105.00 | 61.00–115.00 | 65.00–74.00 | 70.00–86.54 | 82–105 | 73–96;5 |
| HL | 18.80 ± 1.13 | 22.93 ± 1.33 | 21.43 ± 1.21 | 19.67 ± 0.58 | 19.08 ± 1.21 | 22.86 ± 0.69 | 20.6 ± 0.80 |
| | 18.00–19.60 | 21.00–26.00 | 19.00–24.00 | 19.00–20.00 | 17.00–21.00 | 22–24 | 20–22;5 |
| EL | / | 16.03 ± 1.41 | 17.56 ± 1.26 | 17.00 ± 0 | 13.17 ± 1.78 | 17.43 ± 0.53 | 15.4 ± 1.85 |
| | / | 13.50–21.00 | 14.00–20.00 | 17.00–17.00 | 11.00–16.00 | 17–18 | 12–17;5 |
| GLS | 22.20 ± 1.11 | 24.90 ± 1.24 | 23.38 ± 1.17 | 21.55 ± 1.08 | 22.10 ± 0.95 | 25.38 ± 0.77 | 25.01 ± 0.51 |
| | 21.40–23.00 | 23.74–26.33 | 21.65–24.82 | 20.93–22.16 | 20.60–23.43 | 24.48–26.71 | 24.41–25.71;5 |
| CBL | 20.15 ± 1.01 | 22.74 ± 1.14 | 21.26 ± 1.06 | 19.83 ± 0.99 | 20.48 ± 0.88 | 22.34 ± 0.58 | 21.99 ± 0.32 |
| | 19.70–20.60 | 21.39–24.45 | 20.05–22.16 | 19.76–19.89 | 19.21–21.75 | 21.44–23.20 | 21.77–22.28;5 |
| BL | 18.25 ± 0.91 | 20.81 ± 1.04 | 19.46 ± 0.97 | 17.93 ± 0.90 | 18.71 ± 0.27 | 21.16 ± 0.57 | 21.24 ± 0.31 |
| | 17.70–18.80 | 19.50–22.51 | 18.37–20.50 | 17.54–18.31 | 18.28–18.99 | 20.46–21.92 | 20.87–21.73;5 |
| IOB | 4.80 ± 0.24 | 4.99 ± 0.25 | 5.27 ± 0.26 | 4.79 ± 0.24 | 4.75 ± 0.06 | 5.21 ± 0.12 | 5.06 ± 0.19 |
| | 4.70–4.90 | 4.55–5.43 | 5.00–5.60 | 4.77–4.81 | 4.67–4.83 | 4.97–5.35 | 4.78–5.27;5 |
| BCH | 7.70 ± 0.39 | 7.82 ± 0.39 | 7.94 ± 0.40 | 7.11 ± 0.36 | 7.52 ± 0.24 | 8.35 ± 0.37 | 8.37 ± 0.19 |
| | 7.50–7.90 | 7.23–8.91 | 7.35–8.46 | 7.04–7.18 | 7.11–7.88 | 8.03–8.89 | 8.05–8.57;5 |
| ZMW | 11.80 ± 0.59 | 13.86 ± 0.69 | 12.64 ± 0.63 | 11.55 ± 0.58 | 12.48 ± 0.18 | 12.99 ± 0.47 | 13.33 ± 0.24 |
| | 11.40–12.20 | 13.08–15.05 | 12.00–13.39 | 11.35–11.74 | 12.18–12.69 | 12.27–13.52 | 13.08–13.63;4 |
| UML | 3.30 ± 0.17 | 3.81 ± 0.19 | 3.61 ± 0.18 | 3.31 ± 0.17 | 3.74 ± 0.16 | 4.03 ± 0.16 | 4.08 ± 0.06 |
| | 3.20–3.40 | 3.57–4.05 | 3.46–3.85 | 3.13–3.49 | 3.56–4.05 | 3.78–4.21 | 4.00–4.19;5 |
| LUIM | 10.70 ± 0.54 | 12.00 ± 0.60 | 11.34 ± 0.57 | 10.13 ± 0.51 | 10.89 ± 0.24 | 12.38 ± 0.21 | 12.34 ± 0.03 |
| | 10.40–11.00 | 11.42–12.65 | 10.69–12.02 | 10.08–10.17 | 10.61–11.34 | 12.03–12.70 | 12.29–12.37;5 |
| $M^1$-$M^1$ | 5.05 ± 0.25 | 5.57 ± 0.28 | 5.31 ± 0.27 | 4.91 ± 0.25 | 4.90 ± 0.11 | 5.57 ± 0.14 | 5.71 ± 0.06 |
| | 5.00–5.10 | 5.31–5.83 | 5.05–5.52 | 4.80–5.01 | 4.72–5.03 | 5.38–5.74 | 5.65–5.80;5 |
| HCV | 4.05 ± 0.20 | 4.59 ± 0.23 | 3.99 ± 0.20 | 3.96 ± 0.20 | 4.14 ± 0.25 | 4.80 ± 0.14 | 4.85 ± 0.09 |
| | 3.80–4.30 | 4.20–5.06 | 3.60–4.37 | 3.81–4.11 | 3.77–4.52 | 4.5–4.96 | 4.73–4.98;4 |
| LNM-FLM | 5.95 ± 0.30 | 6.76 ± 0.34 | 6.37 ± 0.32 | 5.83 ± 0.29 | 6.03 ± 0.18 | 7.03 ± 0.12 | 7.05 ± 0.17 |
| | 5.60–6.30 | 4.96–7.35 | 6.05–6.57 | 5.79–5.86 | 5.75–6.33 | 6.88–7.20 | 6.82–7.23;4 |

Means (± SD) and ranges of external and cranial measurements. BM: body mass; TL: tail length; HB: head and body length; HL: hind foot length; EL: ear length; GLS: greatest length of skull; CBL: condylobasal length; BL: basal length; IOB: interorbital breadth; BCH: braincase height; ZMW: zygomatic width; UML: upper molar row length; LUIM: length between upper incisor and molar; M1–M1: crown breadth of the first upper molars; HCV: height of coronoid valley; LNM–FLM: length between backmost notch point of mandible and front of lower molars. Missing data are represented by "/". External and cranial morphological measurements of cheekteeth of *T. cinereus*, *T. chapensis*, *T. daloushanensis*, and *T.* nanus were obtained from Cheng et al. (2017); measurements of *T. huangshanensis* were obtained from Hu et al. (2021); measurements of *T. fengjiensis* were obtained from Pu et al. (2022).

**Table 2.** Results and percentage of variance explained by principal component and discriminant function analyses.

| Variables | Component | | Canonical axis 1–3 | | |
|---|---|---|---|---|---|
| | 1 | 2 | 1 | 2 | 3 |
| GLS | 0.951 | –0.027 | 0.114 | 0.445 | –0.030 |
| CBL | 0.882 | –0.180 | –0.050 | –0.779 | 0.511 |
| BL | 0.952 | –0.127 | 0.300 | 0.878 | –0.756 |
| IOB | 0.260 | 0.877 | –0.124 | 0.591 | 0.477 |
| BCH | 0.583 | 0.679 | –0.134 | 0.268 | –0.476 |
| ZMW | 0.847 | –0.230 | –0.091 | –1.357 | 0.421 |
| UML | 0.683 | –0.034 | 0.425 | –0.169 | –0.577 |
| LUIM | 0.955 | –0.032 | 0.136 | 0.408 | 0.473 |
| $M^1$-$M^1$ | 0.903 | 0.126 | 0.351 | 0.316 | 0.579 |
| HCV | 0.810 | –0.331 | 0.419 | –0.155 | –0.673 |
| LNM-FLM | 0.795 | 0.140 | 0.379 | –0.258 | 0.067 |
| Eigenvalues | 7.199 | 1.420 | 10.146 | 5.418 | 3.274 |
| variance explained | 65.448% | 12.906% | 51.5% | 27.5% | 16.6% |

GLS: greatest length of skull; CBL: condylobasal length; BL: basal length; IOB: interorbital breadth; BCH: braincase height; ZMW: zygomatic width; UML: upper molar row length; LUIM: length between upper incisor and molar; $M^1$–$M^1$: crown breadth of the first upper molars; HCV: height of coronoid valley; LNM–FLM: length between backmost notch point of mandible and front of lower molars.

The skull and cheek teeth of *Typhlomys* sp. 1 and *T. daloushanensis* are the most similar: they both have relatively rounded zygomatic arches, the mesofossette on $M^1$ opens on the buccal side only, and the anterofossettes on $M^2$ are present. These characteristics distinguish them from other species within the genus (Cheng et al. 2017; Hu et al. 2021; Pu et al. 2022). However, there are some distinct differences between the two species in the molars: (1) the parafossette on $M^1$ of *Typhlomys* sp. 1 is closed; however, it opens buccally in *T. daloushanensis* (Fig. 5B). (2) In contrast to the anteriorly extended end of the mesofossettid on the $M_1$ in *T. daloushanensis*, that in *Typhlomys* sp. 1 does not extend anteriorly on the buccal side, and the $M_1$ mesofossettid of *Typhlomys* sp. 1 is shorter. (3) *Typhlomys* sp. 1 lacks a prominent buccal extension of the mesolophid on $M_1$.

The three phylogenetic trees reconstructed using Bayesian inference and maximum likelihood analyses exhibited identical topologies (only the BI tree is shown, Fig. 3). These results support that the genus *Typhlomys* is divided into two primary clades. The first clade comprises *T. nanus* and *T. chapensis*. The second clade consists of

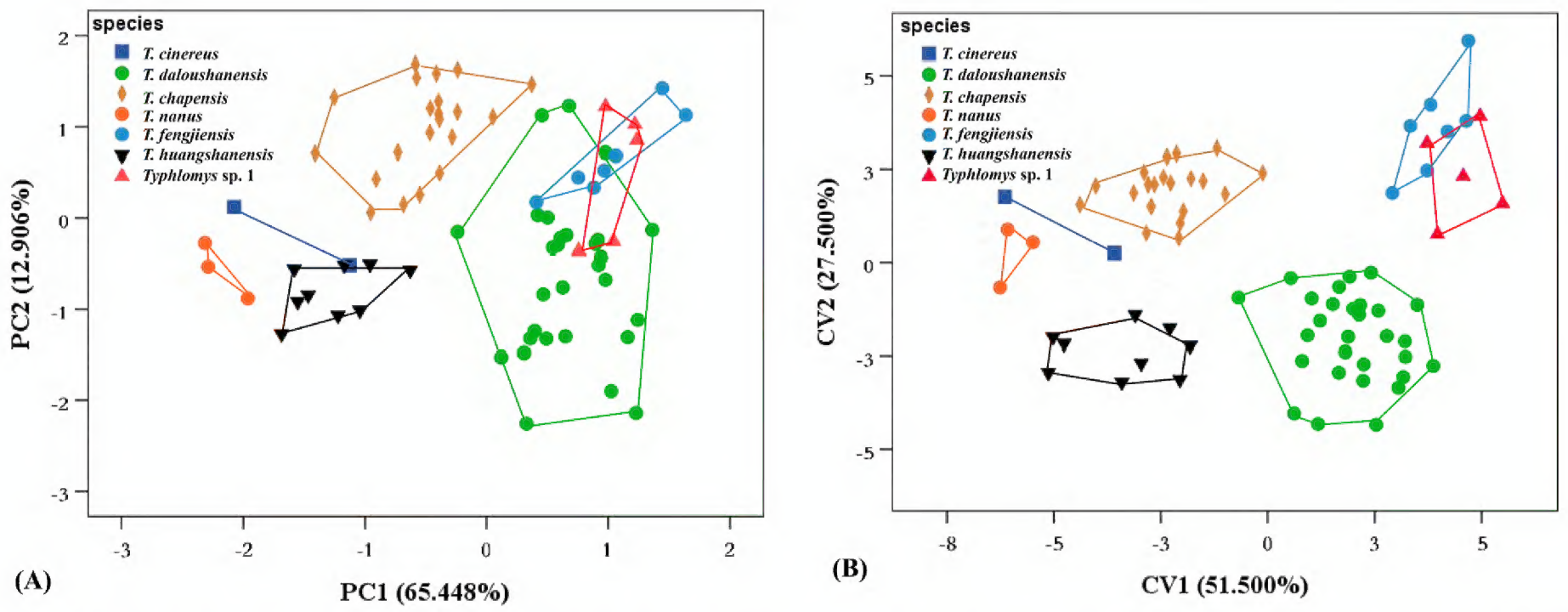


**Figure 2.** Results of principal component analysis (**A**) and discriminant function analysis (**B**) based on the skull measurements of the genus *Typhlomys*.

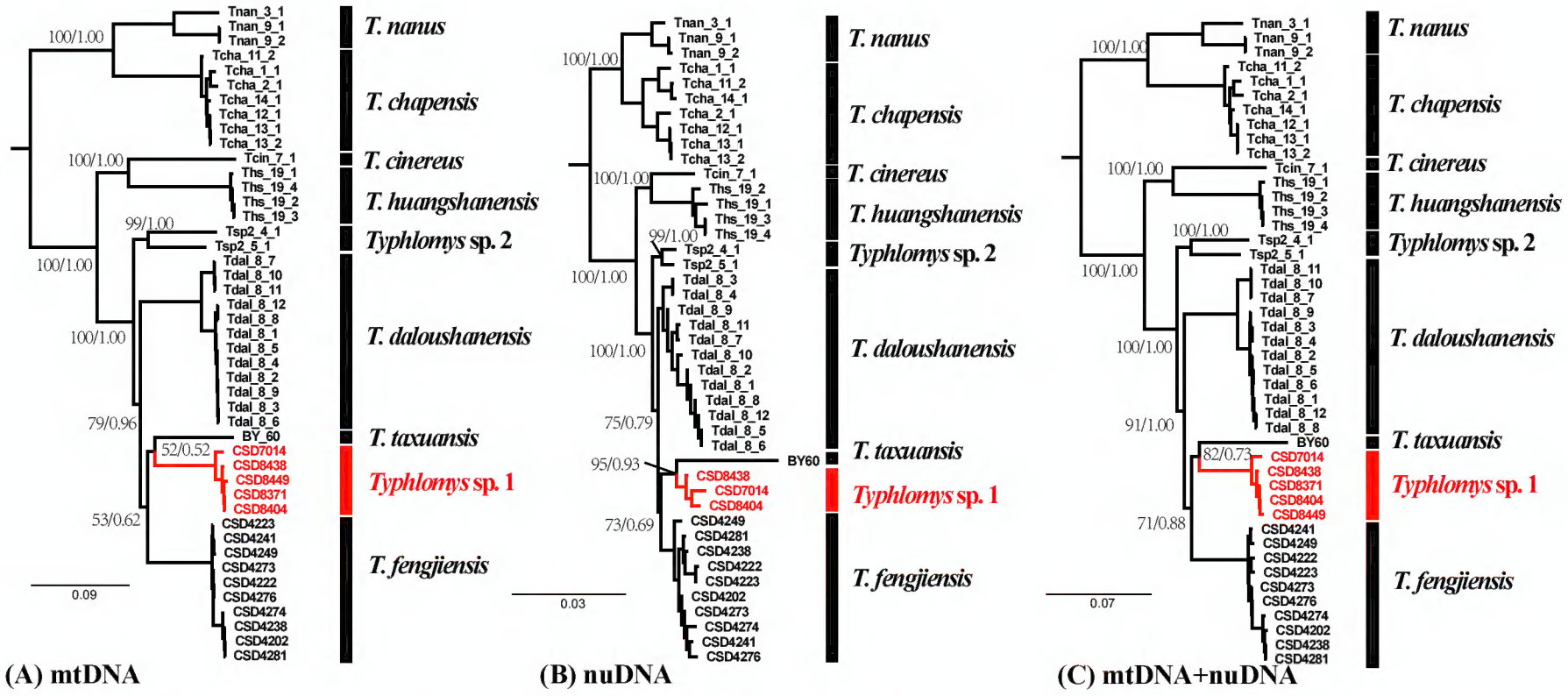


**Figure 3.** Phylogenetic trees of the genus *Typhlomys* based on **A**. Concatenated three mitochondrial genes (*Cytb*, *COI*, and *ND2*, mtDNA dataset); **B**. Concatenated two nuDNA genes (*GHR* and *IRBP*, nuDNA dataset); and **C**. Concatenated mitochondrial and nuclear genes (mtDNA + nuDNA dataset) using ML and BI methods. The node numbers refer to ultrafast bootstrap supports (UFBoot) and Bayesian posterior probabilities (PP). The newly described species, *Typhlomys* sp. 1, is highlighted in red.

*T. cinereus*, *T. huangshanensis*, *T. taxuansis*, *Typhlomys* sp. 1, *Typhlomys* sp. 2, *T. fengjiensis*, and *T. daloushanensis*. In all three trees, the two samples representing *Typhlomys* sp. 2 form a distinct branch, consistent with the results of Cheng et al. (2017), Hu et al. (2021), and Pu et al. (2022), while conflicting with the result of Balakirev et al. (2024). Moreover, the results of all phylogenetic trees support that *Typhlomys* sp. 1 forms a distinct branch and groups as a sister clade to *T. taxuansis*; the branches of *Typhlomys* sp. 1 and *T. taxuansis* are sister groups to *T. fengjiensis*. However, support for these relationships was low across all analyses (PP < 0.95, UFBoot ≤ 95; see Fig. 3).

The Kimura 2-parameter *Cytb* interspecific genetic distances ranged from 0.076 to 0.188 in the genus *Typhlomys* (Suppl. material 3). The smallest and largest genetic distances occurred between *T. taxuansis* and *T. fengjiensis* (7.6%) and *T. cinereus* and *T. nanus* (18.8%), respectively. For *Typhlomys* sp. 1, the distances to all other recognized species ranged from 0.082 to 0.179, which falls within the range of interspecific divergence (Yuri Ph. Kartavtsev 2011). Furthermore, the genetic distance of 0.105 between the two specimens designated as *Typhlomys* sp. 2 (Tsp2-4-1 and Tsp2-4-5) suggests that they may represent two distinct species (Suppl. material 3).

BPP analyses based on both datasets consistently recognized nine putative species, with high posterior probabilities obtained from the nuclear dataset and moderate to high support from the combined mitochondrial and nuclear dataset (Fig. 4; Suppl. material 2). The PTP analysis identified 12 species (Fig. 4), including support for *Typhlomys* sp. 1, *T. chapensis*, *T. cinereus*, *T. huangshanensis*, *T. fengjiensis*, and *T. taxuansis* as separate species. The analysis further split each of *T. nanus*, *Typhlomys* sp. 2, and *T. daloushanensis* into two species, yielding six putative species from these three lineages.

The age of the most recent common ancestor of the genus *Typhlomys* was estimated to be approximately 16.96 Ma (95% CI = 12.59–23.77; Fig. 6). Furthermore,

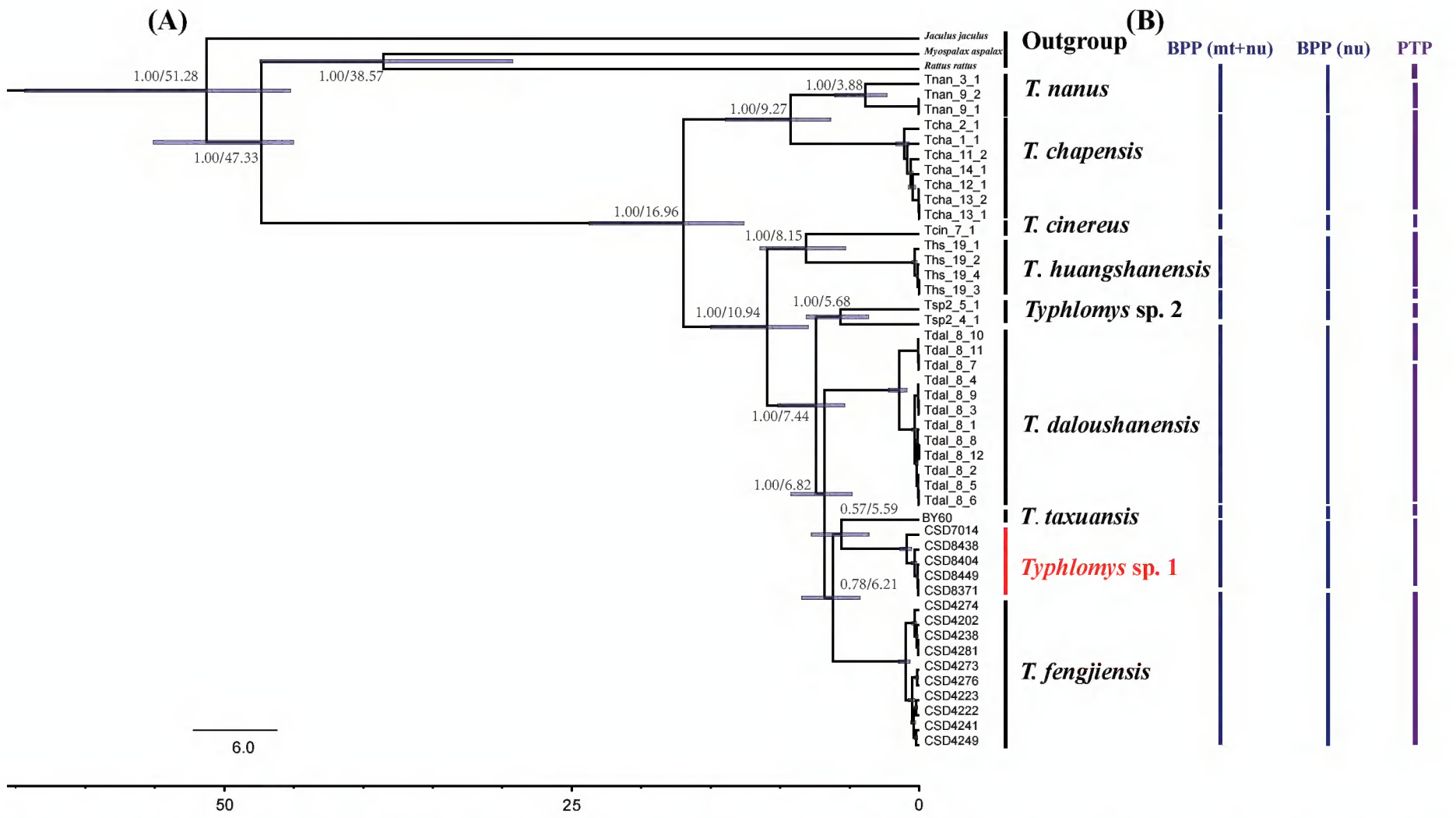


**Figure 4.** Divergence times estimated using BEAST based on the concatenated mtDNA and nuDNA genes (**A**) and species delimitation results (**B**). Branch lengths represent time (Ma). Numbers to the left of the dash represent the posterior probabilities (PP) of each node, and numbers to the right of the dash represent the median divergence time. The newly described species, *Typhlomys* sp. 1, is highlighted in red.

*Typhlomys* sp. 1 and *T. taxuansis* diverged at approximately 5.59 Ma (95% CI = 3.59–7.79), but the posterior probability of the node is low (PP = 0.57; Fig. 4).

Both morphological and molecular analyses indicated species status for *Typhlomys* sp. 1. Thus, we consider *Typhlomys* sp. 1 to be a new species, described below.

## Taxonomy

**Order Rodentia Bowdich, 1821**
**Family Platacanthomyidae Alston, 1876**
**Genus *Typhlomys* Milne-Edwards, 1877**

***Typhlomys zhengkuni* Zhang, Liu & Chen, sp. nov.**
https://zoobank.org/D0F327B3-1FBC-4B65-8CDF-CB7D6E8D7424

**Type material.** ***Holotype*** • SCNU04927 (collection number: CSD 8438), adult male (Fig. 6), collected from Shiyue Huaitai Shu (十月怀胎树 in Chinese) of Fanjing Mountain, Guizhou, China (27.912108°N, 108.675964°E, 2079 m a.s.l.), collected by Tao Zhang, Yu Deng, Qingfang Zou, and Lin Gu on April 2025. The muscle and liver tissues in 95% ethanol, dried skin, and cleaned skull were all deposited in the College of Life Science, Sichuan Normal University, Chengdu, China.

***Paratypes*** • Two adult females, SCNU04860 (collection number: CSD 8371) and SCNU04893 (collection number: CSD 8404), collected in the same locality as the the holotype by Tao Zhang, Yu Deng, Qingfang Zou, and Lin Gu on April 2025. • One adult male, SCNU 04334 (collection number: CSD 7014), collected from Fanjing Mountain, Guizhou, China (27.91936°N, 108.702813°E, 2266.8 m a.s.l.), collected by Siyu Yang, Yu Deng, Qing Liu, and Shuang Liu on 26 March 2024. • One adult female, SCNU 04938 (collection number: CSD 8449), from the eastern side of Fanjing Mountain, collected by Zhengkun Hu in 2024. The above specimens were prepared as dried skins with cleaned skulls and stored at the College of Life Science, Sichuan Normal University.

**Measurements of the holotype (mm).** BM = 25.50 g; HB = 92.00; TL = 122.00; HL = 21.00; EL = 16.00; GLS = 25.49; CBL = 22.25; BL = 21.39; BCH = 8.42; IOB = 5.27; ZMW = 13.08; LUIM = 12.37; UML = 4.08; $M^1$ $M^1$ = 5.65; HCV = 4.98; and LNM-FLM = 7.19.

**Diagnosis.** The new species can be distinguished by its more flattened braincase from *T. nanus* and *T. chapensis*. It has a larger skull and wider zygomatic width than *T. huangshanensis* and *T. cinereus*. In addition, the species further differs from the four species (*T. nanus*, *T. chapensis*, *T. huangshanensis*, and *T. cinereus*) by the anterofossette on $M^2$ being present. In the phylogenetic and PCA analysis, this new species is most closely related to *T. daloushanensis* and *T. fengjiensis*. However, it can be easily distinguished from *T. fengjiensis* by its more rounded zygomatic arch and the mesofossette on $M^1$ (open only on the buccal side). From *T. daloushanensis*, it can be distinguished by its larger overall skull size, closed parafossette on $M^1$, and shorter mesofossettid on $M_1$ whose buccal end does not extend anteriorly.

**Description.** A relatively large species in the genus *Typhlomys* (HB = 84.2 ± 8.52; GLS = 25.01 ± 0.51). The

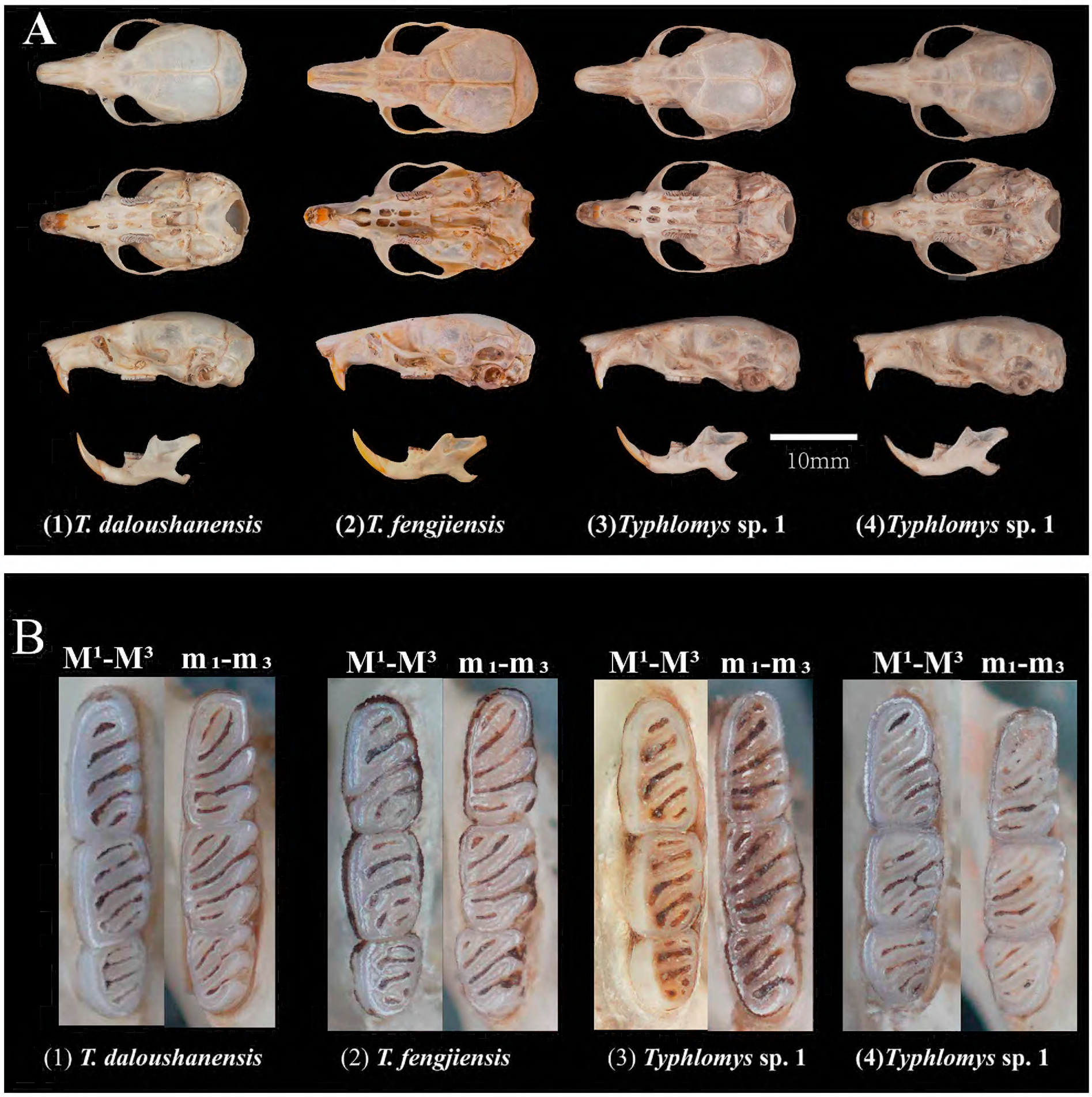


**Figure 5.** Skulls and molar comparisons of *T. daloushanensis*, *T. fengjiensis*, and *Typhlomys* sp. 1. **A.** Ventral, dorsal, and lateral views of the skull and lingual side of mandibles of *T. daloushanensis* (SCNU00558), *T. fengjiensis* (holotype, SCNU02616), and *Typhlomys* sp. 1 (1): female (holotype, SCNU04927, **A**(3)); (2): male (paratype, SCNU04860, **A**(4)); **B.** Molar comparisons of *T. daloushanensis* (SCNU00558), *T. fengjiensis* (holotype, SCNU02616), *Typhlomys* sp. 1 female (SCNU04927, **B**(3)) and *Typhlomys* sp. 1 male (SCNU04860, **B**(4)).

vibrissae are long; the ears are big and almost bare; the hind feet and tail are elongated (HL = 20.6 ± 0.80, TL = 120.40 ± 5.78). The dorsal hair is dark gray with a blackish gray base and a slightly lighter tip. The ventral pelage is slate gray and covered with creamy white hair, distinctly different from the dorsal hair. The cheeks, wrists, and knees are covered with creamy white hair. The palms of the limbs are brown or creamy white, and dorsal surfaces of the hind feet are covered with sparse, short, dark hair. The tail is covered with short hairs in the first third and longer brownish hairs in the rear portion; a tuft of long white hair is present at the tail tip (Fig. 6, Supp. material 5: fig. S1).

The braincase is flattened, and its height is relatively high (BCH = 8.37 ± 0.19). The palatal holes are relatively developed, and three pairs of palatine foramina are present. The dental formula is 1.0.0.3/1.0.0.3 = 16. $M^1$ in all specimens of *Typhlomys zhengkuni* sp. nov. have a relatively wider anteroloph and a narrow posteroloph. The upper molar raw length (UML) is the greatest described in the genus (UML = 4.08 ± 0.06). The parafossette on $M^1$ is closed (but opens buccally in one specimen (SCNU 04893) and the mesofossette on $M^1$ opens on the buccal side only. The anterofossette on $M^2$ is present in 4 of 5 specimens: it is absent in specimen (SCNU 04334) and

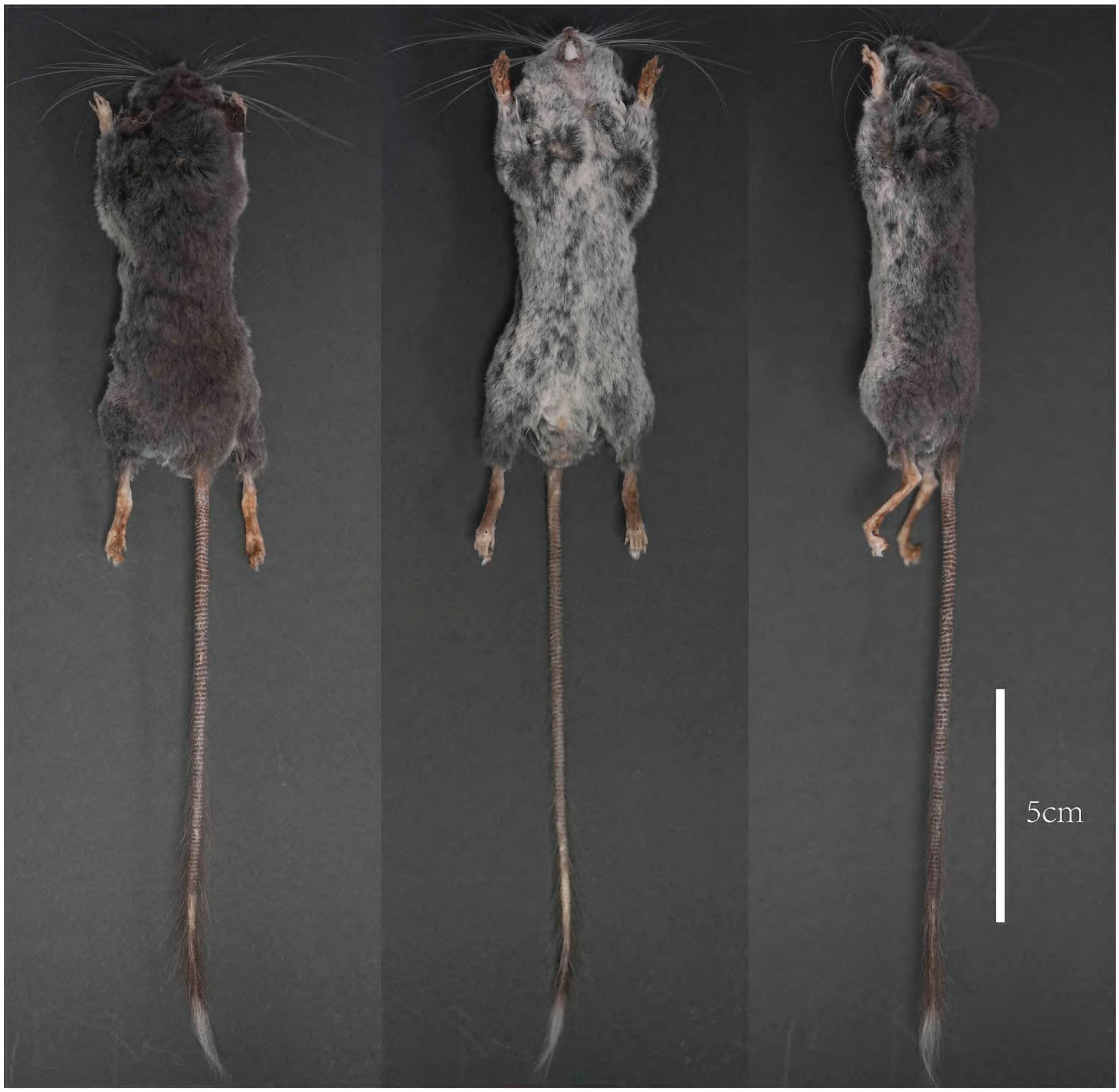


**Figure 6.** Dorsal, ventral, and lateral views of the new species *Typhlomys zhengkuni* sp. nov. (holotype, SCNU04927).

inconspicuous in specimen (SCNU 04860). The $M_1$ anterofossettid is present but inconspicuous in two specimens (SCNU 04334 and SCNU 04860). $M_1$ has a posterossettid and a closed mesofossettid, which is relatively short, and the buccal end does not extend anteriorly. The $M_2$ anterofossettid is present. The third upper and lower molars have three to four fossette-shaped structures (Fig. 5).

**Comparison.** Morphologically, *Typhlomys zhengkuni* sp. nov. is most similar to *T. daloushanensis* but can be distinguished from the latter by larger skull size. Discriminant function analysis based on cranial measurements clearly separates the two species. (Fig. 2B). Moreover, there are significant differences in the morphology of cheek teeth between the two species: The new species has a closed mesofossette on $M^1$, while it is usually opened in *T. daloushanensis*; The mesofossettid on $M_1$ in *Typhlomys zhengkuni* sp. nov. is shorter than that in *T. daloushanensis* and, unlike the latter, does not extend anteriorly on the buccal side; The mesolophid on $M_1$ of *Typhlomys zhengkuni* sp. nov. has no prominent extension on the buccal side and appears square-shaped. (Fig. 5B).

*Typhlomys zhengkuni* sp. nov. can be easily distinguished from *T. nanus* and *T. chapensis* by its more flattened braincase, the anterofossette on $M^2$ being present and the mesofossettid on $M_1$ being closed. Furthermore, it can be distinguished by its larger skull size from *T. nanus*, and all measurements of *Typhlomys zhengkuni* sp. nov. show nearly no overlap with those of *T. nanus* (Table 1). Its creamy white ventral pelage further differs from the yellowish-white ventral pelage of *T. chapensis*.

*Typhlomys zhengkuni* sp. nov. can be distinguished from *T. cinereus* and *T. huangshanensis* by its larger skull and the anterofossette on $M^2$ being present. Besides, it can further be distinguished from *T. huangshanensis* by the mesofossette on $M^1$ (open buccally in *Typhlomys zhengkuni* sp. nov. vs. open on both buccal and lingual

sides in *T. huangshanensis*); from *T. cinereus* by the zygomatic arch (slightly incurved in *Typhlomys zhengkuni* sp. nov. vs. deep incurved in *T. cinereus*).

Compared to *T. taxuansis* and *T. fengjiensis*, *Typhlomys zhengkuni* sp. nov. can be distinguished by the mesofossette on $M^1$, which opens only on the buccal side. In addition, *Typhlomys zhengkuni* sp. nov. has a more rounded zygomatic arch than that of *T. fengjiensis*. (Fig. 5).

**Suggested common name.** We propose "Zhengkun's Blind Mouse" for the English common name and "政坤猪尾鼠" for the Chinese common name.

**Etymology.** The specific epithet *zhengkuni* honors Zhengkun Hu, a forest ranger at Fanjing Mountain, for his valuable contributions to our fieldwork and for providing the specimens of the new species.

**Distribution and ecology.** This new species is known only from Fanjing Mountain in Guizhou Province, China, at elevations of 2079–2266 m. All specimens were captured in the broad-leaved forest belt among moss-covered stone piles, where they occur sympatrically with species including *Sorex bedfordiae*, *Uropsilus gracilis*, *Niviventer lotipes*, *Dremomys pernyi*, *Apodemus nigrus*, *Anourosorex squamipes*, and *Parablarinella griselda*.

## Discussion

Our molecular and morphological analyses confirm the recognition of a new species of *Typhlomys*, bringing the total number of recognized species in the genus to eight. However, the phylogenetic position of the new species described herein remains to be fully resolved. Nodes among three species (*T. fengjiensis*, *T. taxuansis*, and *Typhlomys* sp. 1) in our tree received only low to moderate support, which could be caused by incomplete gene sequences (e.g., *T. taxuansis* was amplified only for *Cytb*, *COI*, and *GHR*) as well as incomplete lineage sorting in recent, rapid radiations (Giarla and Esselstyn 2015). Although the topology of our phylogenetic tree based on concatenated gene fragments is consistent with that reported by Pu et al. (2022), a recent phylogenetic study (Na et al. 2025) using complete mitochondrial genomes of seven species in *Typhlomys* has proposed alternative topologies with higher statistical support. This discrepancy highlights the limitations of using only a few gene fragments. In particular, the conflicting signal observed from the *COI* and *GHR* genes may also have contributed to the reduced nodal support, underscoring the need for genome-scale data to effectively disentangle these evolutionary histories. Therefore, future analyses incorporating complete mitochondrial and genomic data will be essential to definitively resolve the taxonomic status of this new species and to establish a more reliable phylogeny for the genus, an approach further supported by recent taxonomic studies (Wei et al. 2025).

Morphological differentiation among closely related small mammal taxa (e.g., *Sicista* and *Neodon*) is often subtle, and cranial measurements alone may be insufficient to reliably distinguish them, as reflected in the overlap observed in our PCA analysis. The incorporation of additional morphological characters, such as penis morphology, may provide further taxonomic resolution for closely related species (Deng et al. 2025; Wang et al. 2025), underscoring the need for expanded sampling in future studies. Furthermore, the taxonomic status of *T. taxuansis* is currently based on only a single specimen sequence, and future studies should increase sample sizes and integrate molecular and morphological data to confirm its monophyly with the species reported in this study.

Isolated mountain ranges are considered to promote speciation in small mammals (Abramov et al. 2014). Because of the unique physical and environmental factors, Fanjing Mountain has developed a distinct ecological pattern that differs from the surrounding karst environment, functioning as an ecologically isolated island, as described in You et al. (2018). The complex topography of this region, combined with the effect of an ecologically isolated island, may be a key driver of speciation, particularly for small mammals. Nevertheless, studies on small mammal biodiversity in this area remain relatively limited. Conducting comprehensive biodiversity surveys of small mammals on Fanjing Mountain is likely to uncover additional unique lineages.

## Ethics statement

All specimens were obtained in accordance with the guidelines of the American Society of Mammalogists and the laws and regulations of China concerning the protection of wild terrestrial animals (State Council Decree 1992; Sikes and Animal 2016) and the Guidelines for Care and Use of Laboratory Animals at the Ethics Committee at Sichuan Normal University (Chengdu, China).

## Acknowledgments

We thank Yu Deng, Shuang Liu, Jin Wang, Qing Liu, and Siyu Yang for collecting field samples for this study. We are very grateful to the administration of Fanjingshan National Nature Reserve, Guizhou, China, for their valuable help throughout the fieldwork. We thank Yingting Pu and Dr. Zhong-Zheng Chen for providing morphological measurement data.

This work was supported by the National Natural Science Foundation of China (32370496) to Shaoying Liu; the Survey of Wildlife and Plant Resources in Key Regions of Tibet (ZL202203601) to Shaoying Liu; the National Natural Science Foundation of China (32070424; 32570519) to Shunde Chen; and the Natural Science Foundation of Sichuan Province (2025ZNSFSC0277) to Shunde Chen.

## References

Abramov AV, Aniskin VM, Rozhnov VV (2012) Karyotypes of two rare rodents, *Hapalomys delacouri* and *Typhlomys cinereus* (Mammalia, Rodentia), from Vietnam. ZooKeys 164: 41–49. https://doi.org/10.3897/zookeys.164.1785

Abramov AV, Balakirev AE, Rozhnov VV (2014) An enigmatic pygmy dormouse: molecular and morphological evidence for the species taxonomic status of *Typhlomys chapensis* (Rodentia: Platacanthomyidae). Zoological Studies 53: 34. https://doi.org/10.1186/s40555-014-0034-2

Balakirev A, Phuong B, Rozhnov V (2024) *Typhlomys taxuansis* (Rodentia, Platacanthomyidae): new species of the genus from northern Vietnam with notes on conservation status and distribution. Biodiversity Data Journal 12: e133363. https://doi.org/10.3897/BDJ.12.e133363

Bouckaert R, Heled J, Kühnert D, Vaughan T, Wu CH, Xie D, Suchard MA, Rambaut A, Drummond AJ (2014) BEAST 2: A software platform for bayesian evolutionary analysis. PLoS Computational Biology 10(4): e100353. https://doi.org/10.1371/journal.pcbi.1003537

Cheng F, He K, Chen ZZ, Zhang B, Wan T, Li JT, et al. (2017) Phylogeny and systematic revision of the genus *Typhlomys* (Rodentia, Platacanthomyidae), with description of a new species. Journal of Mammalogy 98(3): 731–743. https://doi.org/10.1093/jmammal/gyx016

Chen SD, Tang KY, Wang XM, Li FJ, Fu CK, Liu Y, Faiz AUH, Jiang XL, Liu SY (2022) Multi-locus phylogeny and species delimitations of the striped-back shrew group (Eulipotyphla: Soricidae): implications for cryptic diversity, taxonomy and multiple speciation patterns. Molecular Phylogenetics and Evolution 117: 107619. https://doi.org/10.1016/j.ympev.2022.107619

Deng Y, liu Q, Wang XM et al. (2025) Molecular phylogeny and taxonomy of the Sicista concolor group (Mammalia, Rodentia, Sicistidae) with the description of a new species. Zoosystematics and Evolution (101)3: 1197–1211. https://doi.org/10.3897/zse.101.155510

Giarla TC, Jacob Esselstyn JA (2015) The Challenges of Resolving a Rapid, Recent Radiation: Empirical and Simulated Phylogenomics of Philippine Shrews. Systematic Biology 64(5): 727–740. https://doi.org/10.1093/sysbio/syv029

He K, Liu Q, Xu DM, Qi FY, Bai J, He SW, Chen P, Zhou X, Cai W-Z, Chen Z-Z, Liu Z, Jiang X-L, Shi P (2021) Echolocation in soft-furred tree mice. Science 372. https://doi.org/10.1126/science.aay1513

Huelsenbeck J, Rannala B (2004) Frequentist properties of Bayesian posterior probabilities of phylogenetic trees under simple and complex substitution models. Systematic Biology 53(6): 904–913. https://doi.org/10.1080/10635150490522629

Hu TL, Cheng F, Xu Z, Chen ZZ, Yu L, Ban Q, Li C-L, Pan T, Zhang B-W (2021) Molecular and morphological evidence for a new species of the genus *Typhlomys* (Rodentia: Platacanthomyidae). Zoological Research 42(1): 100–107. https://doi.org/10.24272/j.issn.2095-8137.2020.132

Jiang XL, Hoffmann RS (2001) A revision of the white-toothed shrews (Crocidura) of southern China. Journal of Mammalogy 82: 1059–1079. https://doi.org/10.1644/1545-1542(2001)082<1059:arotwt>2.0.co;2

Kartavtsev YP (2011) Sequence divergence at mitochondrial genes in animals: Applicability of DNA data in genetics of speciation and molecular phylogenetics. Marine Genomics 4(2): 71–81. https://doi.org/10.1016/j.margen.2011.02.002

Kimura M (1980) A simple method for estimating evolutionary rate of base substitutions through comparative studies of nucleotide sequences. Journal of Molecular Evolution 16(2): 111–120. https://doi.org/10.1007/BF01731581

Minh BQ, Trifinopoulos J, Schrempf D, Schmidt HA (2018) IQ-TREE version 1.6.8: Tutorials and Manual. Phylogenomic software by maximum likelihood http://www.iqtree.org

Musser GG, Carleton MD (2005) Superfamily Muroidea. In: Wilson DE, Reeder DM (Eds) Mammal Species of the World: A Taxonomic and Geographic Reference. Baltimore: Johns Hopkins University Press, 894–1531.

Na C, Wang X, Cheng Y, Huang Y, He S, Khanal L, Chen S, Jiang X, Chen Z (2025) Mitogenomic Insights into Phylogeny, Biogeography and Adaptive Evolution of the Genus *Typhlomys* (Rodentia: Platacanthomyidae). Animals 15(19): 2823. https://doi.org/10.3390/ani15192823

Nguyen LT, Schmidt HA, von Haeseler A, Minh BQ (2015) IQ-TREE: A fast and effective stochastic algorithm for estimating maximum-likelihood phylogenies. Molecular Biology and Evolution 32(1): 268–274. https://doi.org/10.1093/molbev/msu300

Pu Y-T, Wan T, Fan R-H, Fu C-K, Tang K-Y, Jiang X-L, Zhang B-W, Hu T-L, Chen S-D, Liu S-Y (2022) A new species of the genus *Typhlomys* Milne-Edwards, 1877 (Rodentia: Platacanthomyidae) from Chongqing, China. Zoological Research 43(3): 413−417. https://doi.org/10.24272/j.issn.2095-8137.2021.338

Rambaut A, Drummond AJ, Xie D, Baele G, Suchard MA (2018) Posterior Summarization in Bayesian Phylogenetics Using Tracer 1.7. Systematic Biology 67(5): 901–904. https://doi.org/10.1093/sysbio/syy032

Rodrigues HG, Marivaux L, Vianey-Liaud M (2010) Phylogeny and systematic revision of Eocene Cricetidae (Rodentia, Mammalia) from Central and East Asia: on the origin of cricetid rodents. Journal of Zoological Systematics and Evolutionary Research 48(3): 259–268. https://doi.org/10.1111/j.1439-0469.2009.00542.x

Ronquist F, Teslenko M, Mark PVD, Ayres DL, Darling A, Höhna S, Larget B, Liu L, Huelsenbeck JP, Suchard MA (2012) MrBayes 3.2: Efficient bayesian phylogenetic inference and model choice across a large model space. Systematic Biology 61(3): 539–542. https://doi.org/10.1093/sysbio/sys029

Smith AT (2008) Family Platacanthomyidae. In: Smith AT, Xie Y. A Guide to the Mammals of China. Changsha: Hunan Education Publishing House, 86–87. [in Chinese]

Su WT, Chen ZZ, Wan T, Wang X, Zhou HY, Hu Y, et al. (2020) Taxonomy and distribution of the genus *Typhlomys* in China based on karyotypic and phylogenetic analyses. *Acta* Theriologica Sinica 40(3): 239–248. [in Chinese] https://doi.org/10.16829/j.slxb.150365

Tamura K, Stecher G, Kumar S (2021) MEGA11: Molecular Evolutionary Genetics Analysis version 11. Molecular Biology and Evolution 38(7): 3022–3027. https://doi.org/10.1093/molbev/msab120

Wang XM, Pan X, Liu YX, Murphy RW, Peng B, Duan C, Liao R, Wang X, Liu S (2025) Three new species of Neodon (Rodentia, Cricetidae) from Sichuan and Xizang, China. Zoosystematics and Evolution 101(3): 999–1012. https://doi.org/10.3897/zse.101.140898

Wang YX, Li CY, Chen ZP (1996) Taxonomy, distribution and differentiation on *Typhlomys cinereus* (Platacanthomyidae, Mammalia). Acta Theriologica Sinica 16(1): 54–66. [in Chinese] https://doi.org/10.16829/j.slxb.1996.01.011

Wei QJ, Cao L, He XC, Abramov A, Wang J, Fu J, Li R, Yang Q-S, Fu L-Q, Huang Y-H, Zhou C-Q, Wen Z-X, Ge D-Y(2025) Phylogenomics of the Genus *Mustela* with description of a new species from China. Journal of Systematics and Evolution 00(0): 1–17. https://doi.org/10.1111/jse.70029

Xia L, Yang QS, Ma Y, Feng ZJ, Zhou LZ (2006) A Guide to the Measurement of Mammal Skull III: Rodentia and Lagomorpha. Chinese Journal of Zoology 41(5): 68–71. [in Chinese] https://doi.org/10.13859/j.cjz.2006.05.013

Yang QS, Xia L, Ma Y, Feng ZJ, Quan GQ (2005) A Guide to the Measurement of Mammal Skull I: Basic Measurement. Chinese Journal of Zoology 40(3): 50–56. [in Chinese] https://doi.org/10.13859/j.cjz.2005.03.011

Yang ZH, Rannala B (2010) Bayesian species delimitation using multilocus sequence data. Proceedings of the National Academy of Sciences 107(20): 9264–9269. https://doi.org/10.1073/pnas.0913022107

You ML, Rong L, Xiong KN, Chen H, Li GC, Zhou YW, Gao XQ, Lin DD (2018) Effect of ecological isolated island of Fanjingshan in Guizhou based on the Comparative Analysis of Spermatophyte Flora, Molecular Plant Breeding 16(24): 8185–8198. [In Chinese] https://doi.org/10.13271/j.mpb.016.008185

Zhang JJ, Kapli P, Pavlidis P, Stamatakis A (2013) A general species delimitation method with applications to phylogenetic placements. Bioinformatics 29(22): 2869–2876. https://doi.org/10.1093/bioinformatics/btt499

Zhang D, Gao FL, Jakovlić I, Zou H, Zhang J, Li WX, Wang GT (2020) PhyloSuite: An integrated and scalable desktop platform for streamlined molecular sequence data management and evolutionary phylogenetics studies. Molecular Ecology Resources 20(1): 348–355. https://doi.org/10.1111/1755-0998.13096

## Supplementary material 1

### Museum number, identification code, GenBank accession numbers, and distributions of samples of *Typhlomys* and outgroups used in this study

Authors: Tao Zhang, Zhengkun Hu, Qingfang Zou, Lin Gu, Wei Zhuang, Pengxi Gu, Jiali Zhan, Xiaoqi Mi, Shaoying Liu, Shunde Chen

Data type: xlsx

Copyright notice: This dataset is made available under the Open Database License (http://opendatacommons.org/licenses/odbl/1.0/). The Open Database License (ODbL) is a license agreement intended to allow users to freely share, modify, and use this Dataset while maintaining this same freedom for others, provided that the original source and author(s) are credited.

Link: https://doi.org/10.3897/zse.102.181212.suppl1

## Supplementary material 2

### Results of Bayesian Phylogenetics and Phylogeography (BPP) analyses based on the concatenated genes (mt + nu) and concatenated nuclear genes using different models, algorithms, and priors within the genus *Typhlomys*

Authors: Tao Zhang, Zhengkun Hu, Qingfang Zou, Lin Gu, Wei Zhuang, Pengxi Gu, Jiali Zhan, Xiaoqi Mi, Shaoying Liu, Shunde Chen

Data type: xlsx

Copyright notice: This dataset is made available under the Open Database License (http://opendatacommons.org/licenses/odbl/1.0/). The Open Database License (ODbL) is a license agreement intended to allow users to freely share, modify, and use this Dataset while maintaining this same freedom for others, provided that the original source and author(s) are credited.

Link: https://doi.org/10.3897/zse.102.181212.suppl2

## Supplementary material 3

### *Cytb* genetic distances within the genus *Typhlomys* calculated using the Kimura 2-parameter model in MEGA 11

Authors: Tao Zhang, Zhengkun Hu, Qingfang Zou, Lin Gu, Wei Zhuang, Pengxi Gu, Jiali Zhan, Xiaoqi Mi, Shaoying Liu, Shunde Chen

Data type: docx

Copyright notice: This dataset is made available under the Open Database License (http://opendatacommons.org/licenses/odbl/1.0/). The Open Database License (ODbL) is a license agreement intended to allow users to freely share, modify, and use this Dataset while maintaining this same freedom for others, provided that the original source and author(s) are credited.

Link: https://doi.org/10.3897/zse.102.181212.suppl3

## Supplementary material 4

### PCR program conditions for mitochondrial cytochrome b, cytochrome c oxidase subunit I, NADH dehydrogenase subunit 2, growth hormone receptor, and interphotoreceptor retinoid-binding protein genes

Authors: Tao Zhang, Zhengkun Hu, Qingfang Zou, Lin Gu, Wei Zhuang, Pengxi Gu, Jiali Zhan, Xiaoqi Mi, Shaoying Liu, Shunde Chen

Data type: docx

Copyright notice: This dataset is made available under the Open Database License (http://opendatacommons.org/licenses/odbl/1.0/). The Open Database License (ODbL) is a license agreement intended to allow users to freely share, modify, and use this Dataset while maintaining this same freedom for others, provided that the original source and author(s) are credited.

Link: https://doi.org/10.3897/zse.102.181212.suppl4

## Supplementary material 5

### Habitat and field images of *Typhlomys zhengkuni* sp. nov. taken by Yu Deng on Fanjing Mountain, Guizhou, China

Authors: Tao Zhang, Zhengkun Hu, Qingfang Zou, Lin Gu, Wei Zhuang, Pengxi Gu, Jiali Zhan, Xiaoqi Mi, Shaoying Liu, Shunde Chen

Data type: docx

Copyright notice: This dataset is made available under the Open Database License (http://opendatacommons.org/licenses/odbl/1.0/). The Open Database License (ODbL) is a license agreement intended to allow users to freely share, modify, and use this Dataset while maintaining this same freedom for others, provided that the original source and author(s) are credited.

Link: https://doi.org/10.3897/zse.102.181212.suppl5

## Supplementary material 6

### Indicators for skull linear analysis used herein

Authors: Tao Zhang, Zhengkun Hu, Qingfang Zou, Lin Gu, Wei Zhuang, Pengxi Gu, Jiali Zhan, Xiaoqi Mi, Shaoying Liu, Shunde Chen

Data type: docx

Copyright notice: This dataset is made available under the Open Database License (http://opendatacommons.org/licenses/odbl/1.0/). The Open Database License (ODbL) is a license agreement intended to allow users to freely share, modify, and use this Dataset while maintaining this same freedom for others, provided that the original source and author(s) are credited.

Link: https://doi.org/10.3897/zse.102.181212.suppl6

## Supplementary material 7

### Phylogenetic analysis based on each individual gene using ML analyses. Node numbers indicate ultrafast bootstrap supports (UFBoot)

Authors: Tao Zhang, Zhengkun Hu, Qingfang Zou, Lin Gu, Wei Zhuang, Pengxi Gu, Jiali Zhan, Xiaoqi Mi, Shaoying Liu, Shunde Chen

Data type: docx

Copyright notice: This dataset is made available under the Open Database License (http://opendatacommons.org/licenses/odbl/1.0/). The Open Database License (ODbL) is a license agreement intended to allow users to freely share, modify, and use this Dataset while maintaining this same freedom for others, provided that the original source and author(s) are credited.

Link: https://doi.org/10.3897/zse.102.181212.suppl7